Ana Clara Rocha Caldeira[1]
Attilio Converti[2]
Moysés Naves de Moraes[3]
Janaína Teles de Faria[1],*

Anthocyanin Partition in Aqueous Two-Phase Systems Based on Isopropanol and Sodium/Ammonium Sulfate

Partitioning of anthocyanins contained in the crude extract of *Syzygium cumini* fruit was investigated in aqueous two-phase systems (ATPS) made up of isopropanol and Na_2SO_4/$(NH_4)_2SO_4$. Na_2SO_4 induced ATPS formation more effectively than $(NH_4)_2SO_4$. The increase in temperature enhanced phase separation in the $(NH_4)_2SO_4$ ATPS, while the opposite occurred in the Na_2SO_4 ATPS. The higher the overall mixture concentration or temperature, the higher the values of tie-line length and slope. In all systems and conditions, anthocyanins preferentially partitioned to the top phase. The partition coefficient and theoretical recovery yield in the top phase varied in the ranges 1.14–1.77 and 53.31–63.87 % in the $(NH_4)_2SO_4$ ATPS, and in the ranges 1.94–21.50 and 65.90–95.55 % in the Na_2SO_4 ATPS.

Keywords: Alcohol-salt system, Anthocyanin partition, Liquid-liquid extraction, Natural pigment, Phase equilibrium

Received: October 16, 2021; *revised:* June 11, 2022; *accepted:* July 12, 2022

DOI: 10.1002/ceat.202100524

1 Introduction

Aqueous two-phase systems (ATPS) have been widely used in separations of biomolecules such as proteins, polypeptides, enzymes [1–6], bioactive compounds [7,8], and natural dyes [9–15], among others. Since both phases are mainly made up of water, they provide mild favorable conditions needed to preserve activities of biomolecules [16]. For this reason, they are increasingly used as an alternative to other extraction methods [11].

Traditionally, ATPS are based on polymer-salt or polymer-polymer [16,17] mixtures, which leads to spontaneous two-phase formation at appropriate concentrations. In recent years, however, other pairs of phase-forming agents have been studied such as alcohol-sugar [18], surfactant-polymer [1], surfactant-ionic liquid [19,20], salt-ionic liquid [14,21], and short-length chain alcohol-salt [22–24]. Systems composed of alcohol-inorganic salt have several advantages over traditional ATPS, among which are lower cost, interfacial tension and viscosity, better resolution, higher yield, simpler scale-up, eco-friendliness [12,14], easy recovery of the target biomolecule from the alcohol-rich phase, and possibility of recycling the phase-forming components [11,25].

Knowledge of ATPS liquid-liquid equilibrium data is essential to design cost-effective processes [26], identify the main factors influencing biomolecule partition, understand the phase behavior of systems, and improve their performance [23].

In the present study, liquid-liquid equilibrium data were obtained for ATPS composed of isopropanol and sodium or ammonium sulfate, and the applicability of these systems to anthocyanin partitioning was investigated. The effects of type of salt, tie-line length, and temperature on the liquid-liquid phase behavior and black plum (*Syzygium cumini*) anthocyanin partitioning were investigated. Anthocyanins, which are considered the most important water-soluble natural pigments [27–29] belonging to the flavonoid group, were chosen as the target biomolecules due to the growing interest of consumers for foods made with healthier and ecofriendly natural ingredients/additives.

2 Materials and Methods

2.1 Preparation of Anthocyanin-Rich Crude Extract

The anthocyanins-rich crude extract was obtained from mature black plum (*Syzygium cumini*) fruits according to Caldeira et al. [9]. After washing and rinsing the fruits, peel (~140 g) was manually recovered and added to 280 mL of HCl solution (pH 2.0) in a 500-mL glass flask protected from light, which

---

[1] Ana Clara Rocha Caldeira, Prof. Dr. Janaína Teles de Faria
janainafaria@ufmg.br
Federal University of Minas Gerais, Agricultural Sciences Institute, Av. Universitária 1000, 39400-000 Montes Claro, Brazil.

[2] Prof. Dr. Attilio Converti
University of Genoa, Department of Civil, Chemical and Environmental Engineering, Pole of Chemical Engineering, Via Opera Pia 15, 16145 Genoa, Italy.

[3] Prof. Dr. Moysés Naves de Moraes
Federal University of Viçosa, Department of Food Technology, Av. P. H. Rolfs, s/n, 36570-900 Viçosa, Brazil.

was then placed in an orbital shaking incubator (Lucadema, São Paulo, Brazil) under 200 rpm stirring for 24 h at 298 K. The extract was filtered through qualitative paper (0.8 µm) and concentrated by lyophilization (Alpha 2-4, Martin Christ, Osterode am Harz, Germany). Aliquots (1.5 mL) of the concentrated extract were kept under freezing (250 K), protected from light, until use.

2.2 Aqueous Two-Phase System Experiments

Binodal curves of systems composed of isopropanol, ammonium or sodium sulfate and water were obtained by the turbidimetric titration method [16] at atmospheric pressure. A 25 wt % stock solution aliquot of the selected salt (~ 1.6 g) was transferred into a glass vial, which was kept in a thermostatic bath at the selected temperature (288, 298 or 308 K). Then, isopropanol was added dropwise (50 µL), followed by fully blending until the clear solution became turbid and separated into two phases spontaneously. Finally, water was added dropwise (50 µL) until the turbidity disappeared. The above procedure was repeated many times to obtain enough data to construct the phase diagrams for either salt. Each phase diagram was obtained in triplicate.

The following equations, which were successful in correlating binodal data of ionic liquid-salt [30, 31], polymer-salt [32, 33], polymer-polymer [4], and alcohol-salt [24, 34] ATPS, were used to fit the ATPS experimental data:

$$[w_1] = A\exp\left(B[w_2]^{0.5} - C[w_2]^3\right) \tag{1}$$

$$[w_1] = A + B[w_2]^{0.5} + C[w_2] \tag{2}$$

$$[w_1] = A + B[w_2]^{0.5} + C[w_2] + D[w_2]^2 \tag{3}$$

$$[w_1] = \exp\left(A + B[w_2]^{0.5} + C[w_2] + D[w_2]^2\right) \tag{4}$$

where $[w_1]$[1] and $[w_2]$ are the total concentrations (wt %) of alcohol and salt, respectively, while *A*, *B*, *C*, and *D* are the regression coefficients.

The correlation with the less root-mean-square error (RMSE) and the highest adjusted determination coefficient (R^2 adj) was chosen to determine each tie-line.

Three different compositions were chosen within the biphasic region of each phase diagram. These systems were prepared by mixing adequate amounts of water, isopropanol, and salt stock solution (25 wt %) to yield a total mass of 10 g. After shaking for 1–2 min, tubes were allowed to settle at the selected temperature for 24 h in a thermostatic water bath to reach equilibrium. The bottom phase was withdrawn using a long needle syringe, and the mass of the top phase was determined gravimetrically, while that of the bottom phase was calculated by mass balance.

Tie-lines were determined applying the lever-arm rule to the relationship between the mass composition of phases and the total system composition [32]. Based on the best correlation equation and lever rule, the phase composition at equilibrium was determined as:

$$[w_1]_\mathrm{m} = \alpha\left([w_1]_\mathrm{b} - [w_1]_\mathrm{m}\right) + [w_1]_\mathrm{t} \tag{5}$$

$$[w_2]_\mathrm{m} = \alpha\left([w_2]_\mathrm{b} - [w_2]_\mathrm{m}\right) + [w_2]_\mathrm{t} \tag{6}$$

where the subscripts m, b, and t indicate the mixture, bottom phase, and top phase, while α is the ratio between bottom phase and top phase masses.

After the compositions at equilibrium had been determined, the tie-line length (*TLL*) and slope (*TLS*) of the different ATPS were calculated as:

$$TLL = \sqrt{\left([w_1]_\mathrm{t} - [w_1]_\mathrm{b}\right)^2 + \left([w_2]_\mathrm{t} - [w_2]_\mathrm{b}\right)^2} \tag{7}$$

$$TLS = \frac{[w_1]_\mathrm{t} - [w_1]_\mathrm{b}}{[w_2]_\mathrm{t} - [w_2]_\mathrm{b}} \tag{8}$$

2.3 Partitioning of Anthocyanins

ATPS were prepared by using the three tie-lines with a volume ratio of the top phase to the bottom phase equal to 1.0 by adding 3 mL of previous equilibrium phases in a glass tube with cap. Thereafter, 100 µL of anthocyanins-rich crude extract were added. Mixtures were shaken vigorously for about 1 min and then placed in a thermostatic water bath at the selected temperature for 15 h. Top and bottom phases were recovered, while the residue at the interface was discarded. Anthocyanin concentration in the collected phases was determined spectrophotometrically as described in Sect. 2.4. Each experiment was carried out in duplicate, and ATPS without anthocyanin were used as controls.

The partition coefficient (*k*) and theoretical recovery yield in the top phase (Y_t) were calculated by the following equations [11, 22]:

$$k = \frac{AC_\mathrm{t}}{AC_\mathrm{b}} \tag{9}$$

$$Y_\mathrm{t}(\%) = \frac{kVR}{1 + (kVR)} \times 100 \tag{10}$$

where AC_t and AC_b are the total anthocyanin concentrations in the top and bottom phases, respectively, and *VR* is the top phase-to-bottom phase volume ratio.

Being in this case *VR* = 1.0, Eq. (10) simplifies to:

$$Y_\mathrm{t}(\%) = \frac{k}{1 + k} \times 100 \tag{11}$$

---

1) List of symbols at the end of the paper.

2.4 Determination of Anthocyanin Content

The total monomeric anthocyanin contents of the top and bottom phases were determined by the pH differential method [35] with some modifications. Briefly, samples were separately diluted in 30 mM KCl buffer (pH 1.0) or 400 mM CH_3COONa buffer (pH 4.5), and let to rest for 30 min. The absorbance (*ABS*) of diluted solutions was read at 520 and 700 nm with a spectrophotometer (UV-1280, Shimadzu, Kyoto, Japan), and the total anthocyanin concentration (*AC*), expressed as cyanidin-3-glucoside, was calculated according to Eq. (12):

$$AC\left[\mathrm{g\ L^{-1}}\right] = \frac{\Delta ABS \times MM \times FD \times 1000}{\varepsilon \times L} \tag{12}$$

where $\Delta ABS = (ABS_{520} - ABS_{700})_{\mathrm{pH1.0}} - (ABS_{520} - ABS_{700})_{\mathrm{pH4.5}}$, *MM* is the molar mass of cyanidin-3-glucoside (449.2 g $\mathrm{mol^{-1}}$), *FD* is the dilution factor, ε is the cyanidin-3-glucoside molar extinction coefficient (26 900 L $\mathrm{cm^{-1} mol^{-1}}$) and *L* is the cuvette light path (1 cm).

The corresponding phases of ATPS without pigment were used as blanks.

3 Results and Discussion

3.1 Binodal Data and Correlation

The binodal curves of the ATPS composed of isopropanol-sodium sulfate and isopropanol-ammonium sulfate at 288, 298, and 308 K are illustrated in Fig. 1. Two regions can be identified: the biphasic region above the curve and the single-phase region below the curve. The closer the binodal curve is to the origin, the larger the biphasic region, the easier the formation of ATPS, and the lower the concentrations of components to get phase separation. Regardless of temperature, the system composed of sodium sulfate showed a larger biphasic region than the other, which implies a greater ability to form ATPS likely due to a higher salting-out effect. The salting-out effect has been related to either cation or anion ionic charge and hydration radius [36]. However, since the salts used in this study share a common anion (SO_4^{2-}), their different ability to induce salting-out can only be ascribed to the different cations, which are well known to influence electrostatic attractions and, consequently, ion solvation.

Khayati and Shahriari [21], who reported for Na^+ and NH_4^+ ion radii of 102 and 148 pm, respectively, observed an increase in salting-out effect with decreasing the cation size. The salting-out effect has also been related to the Gibbs free energy of ion hydration (ΔG_{hyd}), in that, the more negative is ΔG_{hyd}, the more kosmotropic the ion. Since ΔG_{hyd} of Na^+ and NH_4^+ are –365 and –285 kJ $\mathrm{mol^{-1}}$ [37], respectively, both ion radius and ΔG_{hyd} values corroborate the stronger salting-out effect of sodium sulfate compared to ammonium sulfate. Likewise, Wang et al. [36] reported a phase-forming ability of Na_2SO_4 with isopropanol higher than that of $(NH_4)_2SO_4$.

Fig. 1 shows a different influence of temperature on binodal curves of the two ATPS within the investigated range (288–308 K), i.e., a decrease in temperature led to a slight expansion in the two-phase region of the isopropanol-sodium sulfate system, whereas the opposite happened with the other, thus confirming literature findings [23].

The regression coefficients of Eqs. (1)–(4) are listed in Tab. 1 together with the adjusted coefficient of determination (R^2 adj) and root-mean-square error (RMSE). The low values of RMSE (< 0.5095 for $(NH_4)_2SO_4$ ATPS and < 1.3790 for Na_2SO_4 ATPS) and the high values of R^2 adj (> 0.9959 for $(NH_4)_2SO_4$ ATPS and > 0.9777 for Na_2SO_4 ATPS) indicate that all the equations were successful. Therefore, Eqs. (2) and (4) that provided the best fitting for the isopropanol-ammonium sulfate and isopropanol-sodium sulfate systems, respectively, were selected to determine tie-line data.

3.2 Tie-Line Data

Three tie-lines of each system were determined to evaluate the effect of tie-line length (*TLL*) on anthocyanin partition. Phase compositions at equilibrium were obtained by solving Eqs. (5) and (6), along with the following empirical equations corre-

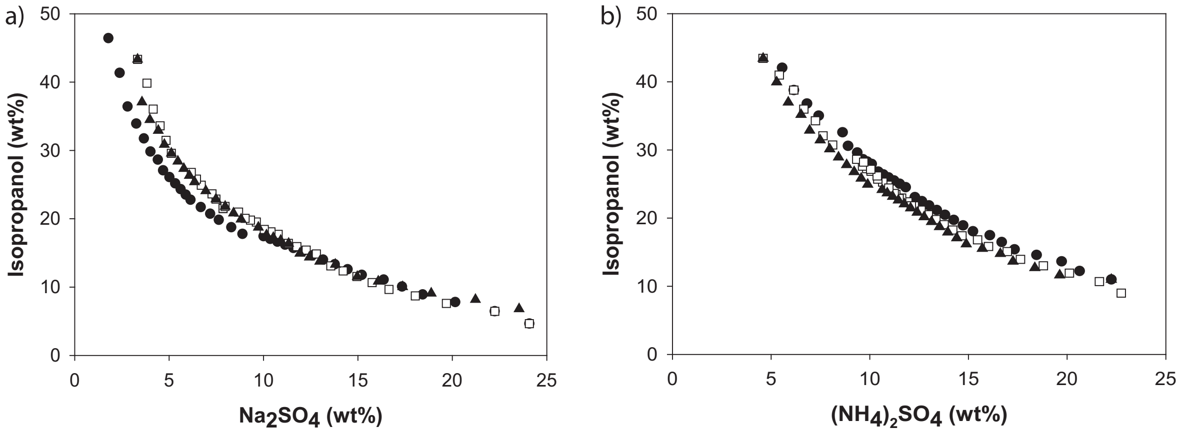

Figure 1. Binodal curves of isopropanol-Na_2SO_4 (a) and isopropanol-$(NH_4)_2SO_4$ (b) aqueous two-phase systems at atmospheric pressure and different temperatures (K): 288 (●), 298 (□), and 308 (▲).

Table 1. Coefficients in Eqs. (1)–(4) estimated by regression of the experimental binodal data of ATPS at different temperatures and pressure of 0.1 MPa, and corresponding values of adjusted determination coefficient (R^2_{adj}) and root-mean-square error (RMSE).

Eq.	Temp. [K]	A	B	C	D	R^2_{adj}	RMSE[a)]
Isopropanol-ammonium sulfate							
1	288	129.0971	−0.47604	0.000022	–	0.9965	0.4641
2	288	99.83535	−30.53331	2.483616	–	0.9966	0.4554
3	288	101.5455	−31.911	2.788135	−0.00411	0.9965	0.4617
4	288	4.667693	−0.34283	−0.02093	−0.00039	0.9965	0.4621
1	298	127.3346	127.3346	0.000026	–	0.9959	0.5095
2	298	98.50025	−30.8074	2.54716	–	0.9965	0.4694
3	298	95.9597	−28.7189	2.078564	0.006419	0.9965	0.4716
4	298	4.226313	0.012871	−0.10627	0.000757	0.9966	0.4636
1	308	133.0247	−0.52237	0.000014	–	0.9959	0.4797
2	308	100.7882	−33.5079	3.038173	–	0.9964	0.4483
3	308	97.87771	−31.0854	2.486641	0.007817	0.9964	0.4501
4	308	4.56582	−0.25652	−0.05743	0.000459	0.9961	0.4666
Isopropanol-sodium sulfate							
1	288	87.72201	−0.52441	3.31×10^{-6}	–	0.9876	1.0302
2	288	70.28326	−24.3396	2.338454	–	0.9777	1.3790
3	288	96.99097	−50.7667	9.136862	−0.11073	0.9950	0.6553
4	288	5.383235	−1.50417	0.273733	−0.00520	0.9980	0.4085
1	298	123.1574	−0.59995	9.896×10^{-6}	–	0.9901	0.9475
2	298	86.51372	−30.8591	2.954518	–	0.9841	1.2014
3	298	120.9847	−61.3164	10.15097	−0.10430	0.9915	0.8788
4	298	6.510887	−2.20557	0.408369	−0.00703	0.9961	0.5920
1	308	1.111	−0.57363	7.337×10^{-7}	–	0.9827	1.1112
2	308	83.14599	−29.7807	2.928411	–	0.9798	1.1991
3	308	99.79112	−44.7255	6.528956	−0.05423	0.9817	1.1423
4	308	5.521843	−1.33700	0.194931	−0.00330	0.9842	1.0599

[a)] $\mathrm{RMSE} = \sqrt{\frac{1}{n}\sum_{i=1}^{n}\left(Y_i - \hat{Y}_i\right)^2}$, where Y_i is the i_{th} experimental concentration of isopropanol, $\hat{Y}_i$ is the i_{th} predicted concentration of isopropanol, and n is the number of binodal data.

sponding to Eqs. (2) and (4) applied to ammonium sulfate and sodium sulfate systems, respectively:

$$[w_1]_t = f\left([w_2]_t\right) \tag{13}$$

$$[w_1]_b = f\left([w_2]_b\right) \tag{14}$$

This methodology was already successful in obtaining liquid-liquid equilibrium data for alcohol, ionic liquid, and polymer-based ATPS [2, 14, 24]. The compositions of overall mixtures and each phase in equilibrium as well as the values of *TLL* and tie-line slope (*TLS*) are listed in Tab. 2 for both ATPS, while the corresponding tie-lines are shown in Fig. 2 as function of temperature.

In all ATPS the alcohol concentration in the top phase was higher than in the bottom one, whereas the opposite occurred with the salt concentration, with the exception of the system consisting of 25 wt % isopropanol and 11.5 wt % ammonium sulfate (Tab. 2). Similar results were obtained for a system composed of 23 wt % isopropanol and 12 wt % ammonium sulfate [26] and for another composed of 25 wt % isopropanol and 8 wt % sodium phosphate dibasic at pH 5 and 298 K [15].

Table 2. Experimental tie-line concentrations (w), together with their respective tie-line length (TLL) and slope (TLS) for isopropanol (1) + ammonium sulfate/sodium sulfate (2) + water systems at different temperatures and pressure of 0.1 MPa.

Temp. [K]	Overall composition		Top phase		Bottom phase		TLL [wt %]	TLS [–]
	w_1 [wt %]	w_2 [wt %]	w_1 [wt %]	w_2 [wt %]	w_1 [wt %]	w_2 [wt %]		
Isopropanol-ammonium sulfate								
288	25.00	13.00	40.82	5.77	16.06	17.09	27.22	–2.19
288	27.00	13.50	47.49	4.24	13.21	19.73	37.62	–2.21
288	29.00	14.00	52.79	3.26	11.25	22.01	45.58	–2.22
298	25.00	11.50	37.08	6.34	18.39	14.32	20.32	–2.34
298	27.00	12.00	45.65	4.28	14.65	17.11	33.55	–2.42
298	29.00	12.50	50.82	3.32	11.98	19.66	42.14	–2.38
308	24.50	12.00	40.99	5.01	15.67	15.74	27.50	–2.36
308	26.50	12.50	46.80	3.84	13.13	18.21	36.61	–2.34
308	28.50	13.00	51.22	3.1	11.38	20.46	43.46	–2.29
Isopropanol-sodium sulfate								
288	21.00	11.00	34.06	3.13	9.48	17.94	28.70	–1.66
288	23.00	13.00	42.92	2.09	6.05	22.29	42.04	–1.83
288	25.00	15.00	51.84	1.48	3.94	25.61	53.63	–1.99
298	23.00	11.00	35.50	4.27	8.48	18.82	30.69	–1.86
298	25.00	13.00	45.75	3.11	5.52	22.29	44.57	–2.10
298	27.00	15.00	53.95	2.54	3.06	26.07	56.07	–2.16
308	23.00	11.00	35.66	4.00	9.50	18.46	29.89	–1.81
308	25.00	13.00	45.17	2.77	6.84	22.21	42.98	–1.97
308	27.00	15.00	53.54	2.10	4.77	25.81	54.23	–2.06

The lower hydrophilicity of alcohol compared to salts may have resulted in a lower solubility in water and its transfer to the top phase [15, 34]. In addition, the higher the isopropanol concentration in the top phase, the higher the water content and ions solvation in the bottom one [35]. This result is in good agreement with literature values for isopropanol-salt ATPS [15, 21, 23, 24, 34, 38].

As for other alcohol-salt ATPS [21, 23, 24, 34], higher alcohol and salt concentrations not only led to a *TLL* increase, with improved partition efficiency, but also made the compositions of top and bottom phases more different from each other. The alcohol concentration in the top phase and that of salt in the bottom one incremented with the increase in the amounts of solutes forming ATPS, resulting in divergent hydrophobicity of the phases in equilibrium. Considering systems with relatively close overall compositions, the values in Tab. 2 also show that the isopropanol concentration in the bottom phase of sodium sulfate ATPS was lower than in that of ammonium sulfate ATPS. This result points to a greater exclusion of alcohol molecules from the salt-rich bottom phase due to the stronger salting-out effect of sodium sulfate.

Higher absolute values of *TLS* were observed for systems containing ammonium sulfate (from –2.42 to –2.19) when compared to those containing sodium sulfate (from –2.16 to –1.66). Taken together, these values are close to those observed for isopropanol-sodium sulfate ATPS at 293 and 303 K [34]. On the other hand, the *TLS* values reported for isopropanol-sodium sulfate ATPS at 298 K [21] were more negative than those obtained in this study, likely due to different system compositions, while those for isopropanol-ammonium sulfate were close.

In general, the higher the *TLL*, the more negative the *TLS* at a given temperature (Tab. 2). *TLS* increased in absolute value with rising temperature up to 298 K and decreased above this threshold value, the only exception being the first tie-line of ammonium sulfate ATPS, in which *TLS* grew within the entire temperature range. Feng et al. [23] reported that a temperature raise from 303 to 333 K resulted in a more negative *TLS* value of isopropanol-ammonium sulfate system, likely due to transfer of water molecules from the top to the bottom phase, with consequent alcohol concentration in the former.

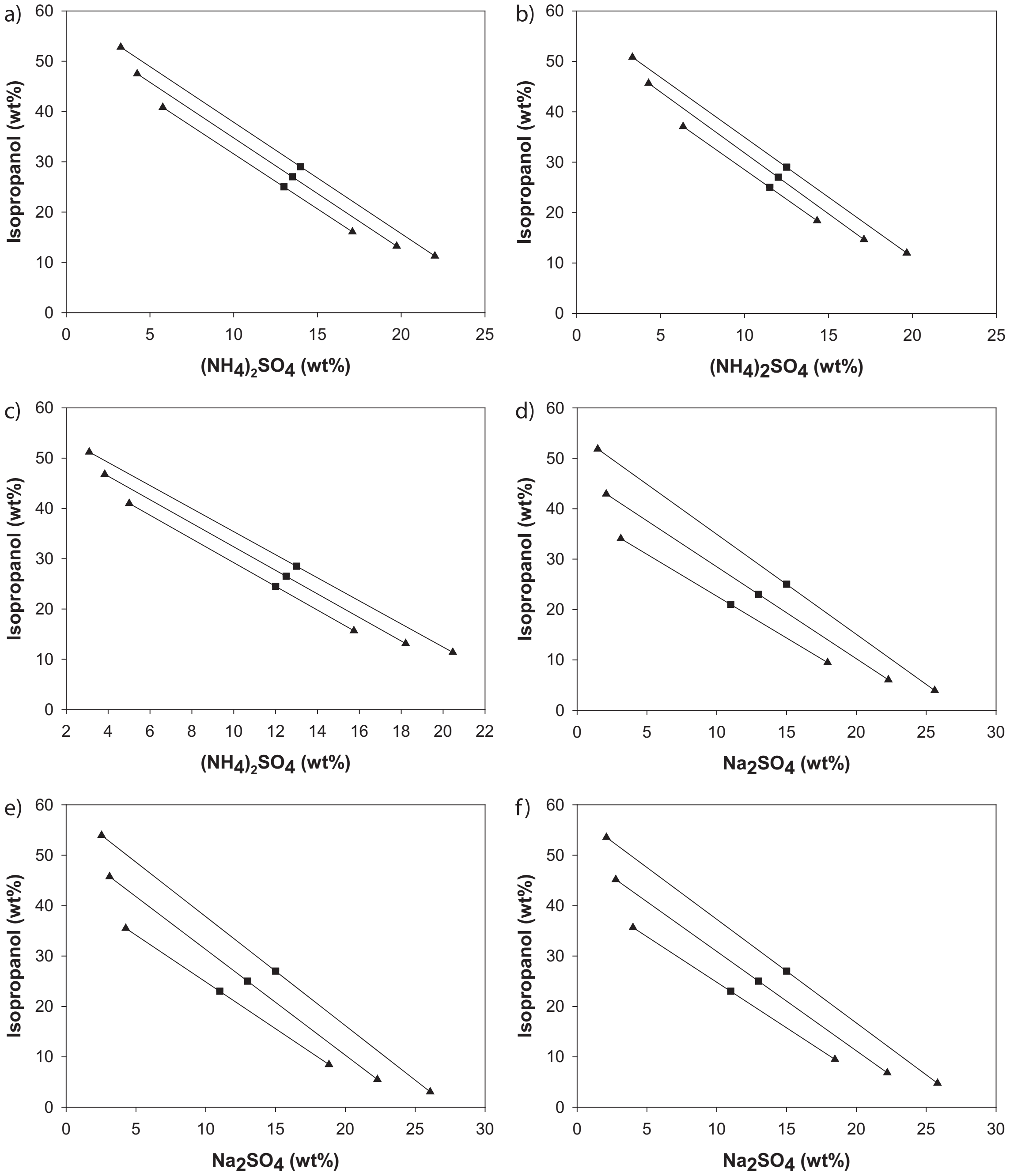

Figure 2. Tie-lines data at different temperatures and atmospheric pressure. Isopropanol-$(NH_4)_2SO_4$ ATPS at 288 K (a), 298 K (b), and 308 K (c). Isopropanol-Na_2SO_4 aqueous two-phase systems at 288 K (d), 298 K (e), and 308 K (f). Tie-line overall composition (■); compositions of actual phases in equilibrium (▲).

3.3 Partitioning of Anthocyanins

Anthocyanins are colored water-soluble pigments belonging to the phenolic group. Besides their use as dyes as well as natural food and beverage colorants, they are also potential pharmaceutical ingredients because of their health benefits such as antioxidant and antimicrobial activities and prevention of chronic diseases [39, 40]. These pigments are commonly found in flowers, vegetables, and fruits, and are extracted as a crude mixture. However, the low extraction yield and high production cost are the main obstacles to their use in the food industry, which has stimulated the search for new sources and extraction/purification methods.

Since partitioning of biomolecules between two phases is influenced by the type of phase-forming compounds, tie-line length, and temperature [34, 41–43], anthocyanin partition in ATPS was performed at different mixture compositions (*TLL*) of each ATPS and different temperatures, whose results are listed in Tab. 3.

All systems showed partition coefficients (k) > 1, which indicates that anthocyanins migrated preferentially to the alcohol-rich top phase. This result, which may be ascribed to the salting-out effect of salt on anthocyanin molecules, agrees with the partitioning preference of anthocyanins for the alcohol phase observed in ethanol-based ATPS [9, 11, 13, 44]. Moreover, it should not be forgotten that the phenolic structure of anthocyanins is responsible for their hydrophobic nature, which makes them soluble in most of the organic solvents [39]. In other words, partitioning of the pigment to the top phase may have been promoted by a combination of salting-out effect, affinity for alcohol, and attractive hydrophobic forces.

The results of Tab. 3 also indicate that an increase in *TLL* favored such a migration. It is known that the higher the *TLL* value, the more the compositions of phases in equilibrium and their intensive properties differ [18]. Particularly, the solubility of biomolecules in the salt-rich bottom phase decreases with increasing salt concentration [3] because the ion-dipole forces between salt ions and water molecules become stronger, thus reducing the amount of free water and promoting the expulsion of both alcohol and biomolecule to the top phase. In addition, as expected by the affinity of anthocyanins for organic solvents [11], the increase in isopropanol concentration in the top phase exalted their partitioning to this phase. Similar results on anthocyanin partition have been reported recently [10, 12, 14].

A raise in temperature from 288 to 308 K led to a k increase in sodium sulfate ATPS from 1.94–3.89 to 7.22–21.50, i.e., favored anthocyanin partitioning to the top phase. On the other hand, temperature had little influence on k in the ammonium sulfate ATPS (1.14–1.77). This trend agrees with the results reported for mulberry anthocyanin partition in ATPS composed of 30 wt % ethanol and 20 wt % ammonium sulfate (2.0–2.3) [27]. In general, the lower k values in the ammonium sulfate ATPS may be ascribed to the acidifying effect of this salt (pH 5.10–5.36) [11], which may have been responsible for protonation of anthocyanins and increased their water solubility [39].

The theoretical recovery yield in the top phase (Y_t) was influenced only by k because the volume ratio of phases was equal to 1 in this study. In general, Y_t increased in both isopropanol-ammonium sulfate and isopropanol-sodium sulfate ATPS with increasing either *TLL* or temperature; however, as for k, the latter ATPS ensured higher Y_t values (65.90–95.55 %) than the former (53.31–63.87 %) and comparable with those (60–80 %) recently reported for anthocyanin recover from *Peristrophe bivalvis* (L.) Merr. leaf using ATPS made up of ethanol and ammonium sulfate [45].

Based on these results, the sodium sulfate ATPS was found to be more suitable than the other for anthocyanin partitioning, ensuring a k value as high as 21.50 with *TLL* of 54.23 wt % at 308 K, which corresponds to a Y_t value of no less than 95.55 %.

4 Conclusions

Liquid-liquid equilibrium data for ATPS formed by isopropanol and sodium sulfate or ammonium sulfate were obtained at 288, 298, and 308 K and atmospheric pressure. Sodium sulfate was more performant than ammonium sulfate to form ATPS under the investigated conditions. A temperature raise favored phase separation in the isopropanol-ammonium sulfate ATPS, whereas the opposite took place in the other. The increased concentration of phase-forming compounds resulted in longer tie-line lengths (*TLL*) and a slightly higher absolute value of tie-line slope. All tested systems and conditions resulted in partition coefficients (k) > 1, indicating that anthocyanins migrated preferentially to the alcohol-rich top phase. The longer the *TLL* or higher the temperature, the higher k and the theoretical recovery yield in the top phase (Y_t), especially in the sodium sulfate-containing ATPS.

The stronger salting-out effect of sodium sulfate over ammonium sulfate significantly favored anthocyanin partitioning and increased the recovery yield. The highest values of k (21.50)

Table 3. Effect of tie-line length (*TLL*) and temperature on anthocyanin partition coefficient (k) and theoretical recovery yield in the top phase (Y_t) at different temperatures and pressure of 0.1 MPa.

Temp. [K]	*TLL* [wt %]	k [–]	Y_t [%]	*TLL* [wt %]	k [–]	Y_t [%]
	Isopropanol-ammonium sulfate			Isopropanol-sodium sulfate		
288	27.22	1.32 ± 0.02	56.86 ± 0.04	28.70	1.94 ± 0.13	65.90 ± 1.53
288	37.62	1.41 ± 0.02	58.47 ± 0.37	42.04	3.82 ± 0.32	79.19 ± 1.40
288	45.58	1.41 ± 0.00	58.56 ± 0.04	52.63	3.89 ± 0.15	79.55 ± 0.64
298	20.32	1.14 ± 0.04	53.31 ± 0.86	30.69	2.25 ± 0.15	69.19 ± 1.40
298	33.55	1.17 ± 0.07	58.83 ± 1.45	44.57	3.06 ± 0.09	75.36 ± 0.52
298	42.14	1.36 ± 0.02	57.60 ± 0.30	56.07	5.07 ± 0.08	83.52 ± 0.21
308	27.50	1.34 ± 0.01	57.28 ± 0.25	29.89	7.22 ± 0.28	87.83 ± 0.41
308	36.61	1.62 ± 0.00	61.82 ± 0.01	42.98	11.81 ± 1.68	92.13 ± 1.03
308	43.46	1.77 ± 0.04	63.87 ± 0.56	54.23	21.50 ± 0.71	95.55 ± 0.14

and Y_t (95.55%) were obtained in the isopropanol-sodium sulfate ATPS with *TLL* of 54.23 wt % at 308 K. The promising tendency of anthocyanins to preferentially partition to the isopropanol-rich top phase suggests that such a system may be industrially used as a preliminary step to recover these thermosensitive pigments by low-pressure evaporation.

Acknowledgment

The authors are thankful to PROBIC-FAPEMIG and PRPq-UFMG for the scholarship granted to the first author and financial support, respectively.

The authors have declared no conflict of interest.

Symbols used

A, B, C, D	[–]	regression coefficients in Eqs. (1)–(4)
ABS	[–]	absorbance
Δ*ABS*	[–]	absorbance difference in Eq. (12)
AC	$[\mathrm{g\,L^{-1}}]$	total concentration of anthocyanins
FD	[–]	dilution factor
ΔG_{hyd}	$[\mathrm{kJ\,mol^{-1}}]$	Gibbs free energy of ion hydration
k	[–]	partition coefficient
L	[cm]	cuvette light path
MM	$[\mathrm{g\,mol^{-1}}]$	molar mass of cyanidin-3-glucoside
R^2	[–]	coefficient of determination
R^2 adj	[–]	adjusted coefficient of determination
RMSE	[–]	less root-mean-square error
TLL	[wt %]	tie-line length
TLS	[–]	tie-line slope
w	[wt %]	total concentration
Y	[%]	theoretical recovery yield

Greek letters

α	[–]	ratio between bottom phase and top phase masses
ε	$[\mathrm{L\,cm^{-1}mol^{-1}}]$	cyanidin-3-glucoside molar extinction coefficient

Subscripts

1	alcohol
2	salt
b	bottom phase
m	mixture
t	top phase

Abbreviation

ATPS	aqueous two-phase system(s)

References

[1] Y. Liu, Y. Zhang, X. Wu, X. Yan, *Fluid Phase Equilib.* **2016**, *429*, 1–8. DOI: https://doi.org/10.1016/j.fluid.2016.08.026

[2] C. A. Suarez Ruiz, C. van den Berg, R. H. Wijffels, M. H. M. Eppink, *Sep. Purif. Technol.* **2018**, *196*, 254–261. DOI: https://doi.org/10.1016/j.seppur.2017.05.001

[3] B. R. Babu, N. K. Rastogi, K. S. M. S. Raghavarao, *Chem. Eng. Process.* **2008**, *47 (1)*, 83–89. DOI: https://doi.org/10.1016/j.cep.2007.08.006

[4] L. S. Castro, P. Pereira, L. A. Passarinha, M. G. Freire, A. Q. Pedro, *Sep. Purif. Technol.* **2020**, *248*, 117051. DOI: https://doi.org/10.1016/j.seppur.2020.117051

[5] X. Chen, W. Diao, Y. Ma, Z. Mao, *RSC Adv.* **2020**, *10*, 29587–29593. DOI: https://doi.org/10.1039/D0RA04245E

[6] M. González-Amado, A. P. M. Tavares, M. G. Freire, A. Soto, O. Rodríguez, *Sep. Purif. Technol.* **2021**, *255*, 117686. DOI: https://doi.org/10.1016/j.seppur.2020.117686

[7] K. Y. Chong, R. Stefanova, J. Zhang, M. S.-L. Brooks, *Sep. Purif. Technol.* **2020**, *252*, 117399. DOI: https://doi.org/10.1016/j.seppur.2020.117399

[8] B. S. Nainegali, R. Iyyaswami, P. D. Belur, *Sep. Sci. Technol.* **2020**, *56 (11)*, 1882–1898. DOI: https://doi.org/10.1080/01496395.2020.1802485

[9] A. C. R. Caldeira, W. F. L. Franca, A. Converti, W. J. N. Lima, F. C. Sampaio, J. T. Faria, *Food Sci. Technol.* **2019**, *39 (Suppl. 2)*, 711–717. DOI: https://doi.org/10.1590/fst.32218

[10] J. Sang, K.-k. Dang, Q. Ma, B. Li, Y.-y. Huang, C.-q. Li, *Food Anal. Methods* **2018**, *11 (4)*, 980–991. DOI: https://doi.org/10.1007/s12161-017-1071-3

[11] Y. Wu, Y. Wang, W. Zhang, J. Han, Y. Liu, Y. Hu, L. Ni, *Sep. Purif. Technol.* **2014**, *124*, 170–178. DOI: https://doi.org/10.1016/J.SEPPUR.2014.01.025

[12] B. Qin, X. Liu, H. Cui, Y. Ma, Z. Wang, J. Han, *Prep. Biochem. Biotechnol.* **2017**, *47 (9)*, 881–888. DOI: https://doi.org/10.1080/10826068.2017.1350980

[13] A. Al-Alawi, R. Nithyanandam, T. L. Hong, Integrated Extraction and Purification of Anthocyanin from Dacryodes rostrata Peel Using Aqueous Two-Phase Extraction (ATPE), *10th EURECA – Int. Eng. Res. Conf.*, Taylor's University, Lakeside Campus, Subang Jaya, Selangor, Malaysia, June **2018**.

[14] B. S. Nainegali, R. Iyyaswami, P. D. Belur, *Food Bioprod. Process.* **2019**, *114*, 185–195. DOI: https://doi.org/10.1016/j.fbp.2019.01.002

[15] I. C. Batista, O. R. R. Gandolfi, V. S. Sampaio, K. A. dos Santos, R. C. I. Fontan, C. M. Veloso, R. C. F. Bonomo, *J. Chem. Technol. Biotechnol.* **2020**, *95 (3)*, 577–584. DOI: https://doi.org/10.1002/jctb.6236

[16] P. A. Albertsson, *Partition of Cell Particles and Macromolecules*, 3rd ed., Wiley Interscience, New York **1986**.

[17] X. Liu, T. Mu, H. Sun, M. Zhang, J. Chen, *Food Chem.* **2013**, *141 (3)*, 3034–3041. DOI: https://doi.org/10.1016/j.foodchem.2013.05.119

[18] N. Ebrahimi, R. Sadeghi, *J. Chromatogr. A* **2018**, *1581–1582*, 156–167. DOI: https://doi.org/10.1016/j.chroma.2018.11.007

[19] S. J. B. Silva, G. M. D. Ferreira, L. R. Lemos, G. D. Rodrigues, A. B. Mageste, *J. Chem. Eng. Data* **2019**, *64 (4)*, 1632–1639. DOI: https://doi.org/10.1021/acs.jced.8b01191

[20] X. Lu, Z. Lu, R. Zhang, L. Zhao, H. Xie, *J. Mol. Liq.* **2021**, *330*, 115677. DOI: https://doi.org/10.1016/j.molliq.2021.115677

[21] G. Khayati, M. Shahriari, *Chem. Biochem. Eng. Q.* **2016**, *30 (1)*, 73–80. DOI: https://doi.org/10.15255/CABEQ.2015.2308

[22] N. E. C. Cienfuegos, P. L. Santos, A. R. García, C. M. F. Soares, A. S. Lima, R. L. Souza, *Food Bioprod. Process.* **2017**, *106*, 1–10. DOI: https://doi.org/10.1016/j.fbp.2017.08.005

[23] Z. Feng, J. Q. Li, X. Sun, L. Sun, J. Chen, *Fluid Phase Equilib.* **2012**, *317*, 1–8. DOI: https://doi.org/10.1016/j.fluid.2011.12.023

[24] W. Guo, J. Ma, Y. Wang, J. Han, Y. Li, S. Song, *Thermochim. Acta* **2012**, *546*, 8–15. DOI: https://doi.org/10.1016/J.TCA.2012.07.022

[25] Y. Wang, J. Han, X. Xu, S. Hu, Y. Yan, *Sep. Purif. Technol.* **2010**, *75 (3)*, 352–357. DOI: https://doi.org/10.1016/J.SEPPUR.2010.09.004

[26] G. Khayati, A. Gholitabar, *J. Chem. Eng. Data* **2016**, *61 (4)*, 1454–1461. DOI: https://doi.org/10.1021/acs.jced.5b00771

[27] X. Wu, L. Liang, Y. Zou, T. Zhao, J. Zhao, F. Li, L. Yang, *Food Chem.* **2011**, *129 (2)*, 443–453. DOI: https://doi.org/10.1016/j.foodchem.2011.04.097

[28] J. He, M. M. Giusti, *Annu. Rev. Food Sci. Technol.* **2010**, *1*, 163–187. DOI: https://doi.org/10.1146/annurev.food.080708.100754

[29] E. Backes, M. G. Leichtweis, C. Pereira, M. Carocho, J. C. M. Barreira, A. K. Genena, I. J. Baraldi, M. F. Barreiro, L. Barros, I. C. F. R. Ferreira, *Food Chem.* **2020**, *333*, 127457. DOI: https://doi.org/10.1016/j.foodchem.2020.127457

[30] P. H. S. Calhau, R. C. S. Sousa, I. J. B. Santos, S. M. Silva, J. S. R. Coimbra, *J. Chem. Eng. Data* **2019**, *64 (9)*, 3781–3785. DOI: https://doi.org/10.1021/acs.jced.9b00055

[31] J. Han, Y. Wang, C. Yu, Y. Li, W. Kang, Y. Yan, *J. Chem. Therm.* **2012**, *45 (1)*, 59–67. DOI: https://doi.org/10.1016/j.jct.2011.09.004

[32] J. C. Merchuk, B. A. Andrews, J. A. Asenjo, *J. Chromatogr. B* **1998**, *711 (1–2)*, 285–293. DOI: https://doi.org/10.1016/S0378-4347(97)00594-X

[33] M. Hu, Q. Zhai, Y. Jiang, L. Jin, Z. Liu, *J. Chem. Eng. Data* **2004**, *49 (5)*, 1440–1443. DOI: https://doi.org/10.1021/je0498558

[34] J. G. Pimentel, S. F. Bicalho, O. R. R. Gandolfi, L. A. A. Verissimo, S. S. Castro, E. A. Souza, C. M. Veloso, R. C. I. Fontan, V. S. Sampaio, R. C. F. Bonomo, *Fluid Phase Equilib.* **2017**, *450*, 184–193. DOI: https://doi.org/10.1016/j.fluid.2017.08.001

[35] T. Fuleki, F. J. Francis, *J. Food Sci.* **1968**, *33 (1)*, 72–77. DOI: https://doi.org/10.1111/j.1365-2621.1968.tb00887.x

[36] Y. Wang, J. Wang, J. Han, S. Hu, Y. Yan, *Cent. Eur. J. Chem.* **2010**, *8 (4)*, 886–891. DOI: https://doi.org/10.2478/s11532-010-0053-8

[37] Y. Marcus, *J. Chem. Soc. Faraday Trans.* **1991**, *87 (18)*, 2995–2999. DOI: https://doi.org/10.1039/FT9918702995

[38] E. Nemati-Knade, H. Shekaari, S. A. Jafari, *Fluid Phase Equilib.* **2012**, *321*, 64–72. DOI: https://doi.org/10.1016/j.fluid.2012.02.015

[39] H. E. Khoo, A. Azlan, S. T. Tang, S. M. Lim, *Food Nutr. Res.* **2017**, *61 (1)*, 1361779. DOI: https://doi.org/10.1080/16546628.2017.1361779

[40] H. Y. Leong, P. L. Show, M. H. Lim, C. W. Ooi, T. C. Ling, *Food Rev. Int.* **2018**, *34 (5)*, 463–482. DOI: https://doi.org/10.1080/87559129.2017.1326935

[41] G. A. Borges, L. P. Silva, J. A. Penido, L. R. de Lemos, A. B. Mageste, G. D. Rodrigues, *J. Environ. Manage.* **2016**, *183 (1)*, 196–203. DOI: https://doi.org/10.1016/j.jenvman.2016.08.056

[42] A. Chakraborty, K. Sen, *J. Chromatogr. A* **2016**, *1433*, 41–55. DOI: https://doi.org/10.1016/j.chroma.2016.01.016

[43] J. Chandrasekhar, K. S. M. S. Raghavarao, *Chem. Eng. Commun.* **2015**, *202 (10)*, 1368–1379. DOI: https://doi.org/10.1080/00986445.2014.935351

[44] Z. Hua, M. Li, *J. Chromatogr. Sep. Tech.* **2013**, *4 (2)*, 1000167. DOI: https://doi.org/10.4172/2157-7064.1000167

[45] P. H. Le, D. N. Dao, T. Q. Huynh, T. T. T. Tran, V. Nguyen, *Nat. Prod. Res.* **2022**, in press. DOI: https://doi.org/10.1080/14786419.2021.1952203